Supplemental Figure Legends

Figure S1: Sas3 and Yng1 colocalize genome wide. A. Scatter plot of Yng1 (Taverna *et al.* 2006) and Sas3 enrichment on 500 bp windows, stepping in 250 bp increments genome wide.

Figure S2. Sas3 is enriched on sense RNAPII-transcribed genes. A. Average profiles for NET-seq (Churchman and Weissman 2011) and Sas3 relative to 4701 +1 nucleosome for genes split into quartiles of enrichment of NET-seq signal. Each gene is only included in the average calculation until its polyadenylation signal. The grey line represents the fraction of genes still contributing to the average profile.

Figure S3: Yng1 is enrichment at methylated nucleosomes. Yng1 (Taverna *et al.* 2006) enrichment at nucleosome positions enriched or depleted for H3K4me1/2/3 and H3K36me3. Yng1 replicate is indicated by colour.

Figure S4: Histone methylation and Sas3 at candidate genes. Input-normalized Sas3 and histone methylation ChIP-seq coverage at *LOS1, SEC15, NUP145,* and *PUT4* genes. ChIP-qPCR amplicons are indicated by red bars on schematic. ChIP-seq data for histone methylation is from (Weiner *et al.* 2015) and (Sadeh *et al.* 2016).

Figure S5: H3K4me3 decreases at *RPS28A* when H3K36 methylation is disrupted. H3K4me3 from wild type and H3K36R strains was quantitatively compared by competitive immunoprecipitation (data from Sadeh *et al.* 2016). The amount of H3K4me3 in wild type and H3K36R at 5' qPCR loci (+100 bp on either side to account for change in resolution) was determined, and the change in methylation is plotted.

Figure S6: H3K14ac and H3K23ac are enriched 5' of Sas3. The average enrichment relative to 4701 +1 nucleosomes for Sas3, H3K14ac, and H3K23ac. H3K14ac and H3K23ac data is from (Weiner *et al.* 2015). Each gene is only included in the average calculation until its polyadenylation signal. The fractions of genes still contributing to the average profile are represented by the gray line.

Figure S7: Modest association between Gcn5 or Sas3 and H3K23ac. Nucleosome enrichments of H3K23ac before and after TSA treatment split by Sas3 (A) or Gcn5 (B) quartiles and by position relative to the TSS. Gcn5 data is from (Xue-Franzén *et al.* 2013). Nucleosomes from cell-cycle regulated genes were excluded, leaving 33942 nucleosomes from +1 to +10 positions relative to the TSS. Outliers were not plotted.

Figure S8: Gcn5 and Sas3 enrichment together does not dictate H3K23ac. Nucleosomes were classified as being enriched or depleted based on being the top or bottom quartile of HAT occupancy respectively. Nucleosomes were grouped as being depleted or enriched for both of Gcn5 or Sas3, enriched for one but not the other, and for not being in one of the above categories. Sas3, Gcn5, and H3K23ac

before and after TSA treatment enrichments for each category were visualized by boxplot. Outliers were not plotted. Gcn5 data is from (Xue-Franzén *et al.* 2013).

Table S1: Published *in vitro* dissociation constants for NuA3 and MOZ/MORF histone-PTM binding domains.

Table S2: Strains

Table S3: ChIP-qPCR primers

Table S4: Nucleosome Spearman correlation coefficients.

Table S1: Published *in vitro* dissociation constants for NuA3 and MOZ/MORF histone-PTM binding domains.

Domain	Peptide	K_D (μM)	Reference
Yng1 PHD finger	H3K4me3	2.3 +/- 0.9, 9.1 +/- 1.6	(Shi *et al.* 2007), (Taverna *et al.* 2006)
	H3K4me2	21.4 +/- 3.0	(Taverna *et al.* 2006)
	H3K4me1	50.7 +/- 7.6	(Taverna *et al.* 2006)
	H3K4me0	>400	(Taverna *et al.* 2006)
Pdp3 PWWP	H3K36me3	69.5 +/- 3.7	(Gilbert *et al.* 2014)
	H3K36me2	414 +/- 23	(Gilbert *et al.* 2014)
	H3K36me1	>1000	(Gilbert *et al.* 2014)
	H3K36me0	>1000	(Gilbert *et al.* 2014)
	H3K79me3	434 +/- 49	(Gilbert *et al.* 2014)
	H4K20me3	> 1000	(Gilbert *et al.* 2014)
Taf14 YEATS	H3K9ac	150.6 +/- 14.5	(Shanle *et al.* 2015)
	H3K9,14,18ac	49.9 +/- 2	(Shanle *et al.* 2015)
	H3K9cr	9.5 +/- 0.5	(Andrews *et al.* 2016)
ING5 PHD finger	H3K4me3	2.4 +/- 1.0	(Champagne *et al.* 2008)
	H3K4me2	16 +/- 1.2	(Champagne *et al.* 2008)
	H3K4me1	222 +/- 17	(Champagne *et al.* 2008)
	H3K4me0	261 +/- 34	(Champagne *et al.* 2008)
BRPF1 PWWP	H3K36me3	2700 +/- 200, 2900 - 4000	(Vezzoli *et al.* 2010), (Wu *et al.* 2011)
	H3K36me2	very weak	(Wu *et al.* 2011)
	H3K36me0	NB	(Wu *et al.* 2011)
	H3K4me3	NB	(Wu *et al.* 2011)
	H3K79me3	very weak	(Wu *et al.* 2011)
	H3K9me3	NB	(Wu *et al.* 2011)

Table S2: Strains

Strain	Parent	Mating type	Genotype	Source
YLH101	FY602	Mat a	*his3D200 leu2D1 lys2-128d ura3-52 trp1D63*	
YVM138	YLH101	Mat a	*his3D200 leu2D1 lys2-128d ura3-52 trp1D63 SAS3-6HA::TRP*	
YVM142	YLR008 x YLH354	Mat a	*his3D200 leu2D1 lys2-128d ura3-52 trp1D63 SAS3-6HA::HIS set1Δ::KANMX6 set2Δ::TRP*	
YVM147	YVM144	Mat a	*his3D200 leu2D1 lys2-128d ura3-52 trp1D63 SAS3-6HA::TRP yng1ΔPHD::KANMX6*	
YVM157	YVM146	Mat a	*his3D200 leu2D1 lys2-128d ura3-52 trp1D63 SAS3-6HA::TRP set1Δ::HISMX6*	
YVM158	YVM146	Mat a	*his3D200 leu2D1 lys2-128d ura3-52 trp1D63 SAS3-6HA::TRP set2Δ::HISMX6*	
YVM207	YVM146	Mat a	*his3D200 leu2D1 lys2-128d ura3-52 trp1D63 SAS3-6HA::TRP ylr455w::HIS*	
YLH696	YVM147	Mat a	*his3D200 leu2D1 lys2-128d ura3-52 trp1D63 SAS3-6HA::TRP yng1DPHD::KANMX6 ylr455w::HISMX6*	
YLH787	YLH101	Mat a	*his3D200 leu2D1 lys2-128d ura3-52 trp1D63 bar1::KAN*	
FY2173		*MAT*α	*his3Δ200 leu2Δ1 lys2-128Δ trp1Δ63 ura3-52 kanMX-GAL1pr-FLO8-HIS3*	(Cheung *et al.* 2008)
L1106		Mat a	*his3Δ200 ura3Δ0 kanMX-GAL1pr-FLO8-HIS3 rco1Δ0::kanMX*	(Cheung *et al.* 2008)
YLH510	L1106	Mat a	*his3Δ200 ura3Δ0 kanMX-GAL1pr-FLO8-HIS3 rco1Δ0::kanMX sas3::URA3*	

Table S3: ChIP-qPCR primers

qPCR primer	Sequence (5' to 3')
NUP145 s+3214	GTATCTTCTGCTGCCTTGTCATC
NUP145 a+3335	CGAAGGAAACTAGCGATGAGG
NUP145 a+1611	CATTGGTTTGGTGGCTTCGTC
NUP145 s+1488	CAACATGATGTGGATCTCACAGC
NUP145 a+281	GTAGCGCCAAATAAGCCACC
NUP145 s+148	CTTCAACACCTAGCCCATCTGG
SEC15 a+2230	GACCCATGAATTGTCTCGTCAAGG
SEC15 s+2082	GTAAGGCAAGACCCGGATATCTC
SEC15 a+1312	GTGACAACCTGTCCATGAGTC
SEC15 s+1092	GGTACAGGTACTACTCCTGGATC
SEC15 a+370	GCACCATACCTTGGATGTTTGC
SEC15 s+230	GGACCCCGTAATTGATGAATTGG
LOS1 a+1395	CAGACTTGGGTCAATTACCACG
LOS1 a+2940	GTCGTCATTATCCAAGCAGGTCC
LOS1 s+2831	CTATACGCCGCAAGAGATCCAG
LOS1 s+1301	GGTCACACAGGATGATTTTGAGG
LOS1 a+230	CCATTTGGATTAGCGTTCACGC
LOS1 s+69	CAAGCCATCGAGCTGCTAAATG
PUT4 a+714	CACGCATAGAAAGATCGTGATCC
PUT4 s+546	CTGGTCACTAGGTACGTTGAC
RPS28A s + 15	CCAGTCACTTTAGCCAAGGTC
RPS28A a +191	CGAGCTTCACGTTCAGATTCC

Supplemental References:

Andrews F. H., Shinsky S. A., Shanle E. K., Bridgers J. B., Gest A., Tsun I. K., Krajewski K., Shi X., Strahl B. D., Kutateladze T. G., 2016 The Taf14 YEATS domain is a reader of histone crotonylation. Nature Chemical Biology **12**: 396–398.

Champagne K. S., Saksouk N., Peña P. V., Johnson K., Ullah M., Yang X.-J., Côté J., Kutateladze T. G., 2008 The crystal structure of the ING5 PHD finger in complex with an H3K4me3 histone peptide. Proteins **72**: 1371–1376.

Cheung V., Chua G., Batada N. N., Landry C. R., Michnick S. W., Hughes T. R., Winston F., 2008 Chromatin- and transcription-related factors repress transcription from within coding regions throughout the Saccharomyces cerevisiae genome. PLoS

Biol **6**: e277.

Churchman L. S., Weissman J. S., 2011 Nascent transcript sequencing visualizes transcription at nucleotide resolution. Nature **469**: 368–373.

Gilbert T. M., McDaniel S. L., Byrum S. D., Cades J. A., Dancy B. C. R., Wade H., Tackett A. J., Strahl B. D., Taverna S. D., 2014 A PWWP domain-containing protein targets the NuA3 acetyltransferase complex via histone H3 lysine 36 trimethylation to coordinate transcriptional elongation at coding regions. Mol. Cell Proteomics **13**: 2883–2895.

Sadeh R., Launer-Wachs R., Wandel H., Rahat A., Friedman N., 2016 Elucidating Combinatorial Chromatin States at Single-Nucleosome Resolution. Molecular Cell: 1–24.

Shanle E. K., Andrews F. H., Meriesh H., McDaniel S. L., Dronamraju R., DiFiore J. V., Jha D., Wozniak G. G., Bridgers J. B., Kerschner J. L., Krajewski K., Martín G. M., Morrison A. J., Kutateladze T. G., Strahl B. D., 2015 Association of Taf14 with acetylated histone H3 directs gene transcription and the DNA damage response. Genes Dev. **29**: 1795–1800.

Shi X., Kachirskaia I., Walter K. L., Kuo J.-H. A., Lake A., Davrazou F., Chan S. M., Martin D. G. E., Fingerman I. M., Briggs S. D., Howe L., Utz P. J., Kutateladze T. G., Lugovskoy A. A., Bedford M. T., Gozani O., 2007 Proteome-wide analysis in Saccharomyces cerevisiae identifies several PHD fingers as novel direct and selective binding modules of histone H3 methylated at either lysine 4 or lysine 36. J. Biol. Chem. **282**: 2450–2455.

Taverna S. D., Ilin S., Rogers R. S., Tanny J. C., Lavender H., Li H., Baker L., Boyle J., Blair L. P., Chait B. T., Patel D. J., Aitchison J. D., Tackett A. J., Allis C. D., 2006 Yng1 PHD finger binding to H3 trimethylated at K4 promotes NuA3 HAT activity at K14 of H3 and transcription at a subset of targeted ORFs. Molecular Cell **24**: 785–796.

Vezzoli A., Bonadies N., Allen M. D., Freund S. M. V., Santiveri C. M., Kvinlaug B. T., Huntly B. J. P., Göttgens B., Bycroft M., 2010 Molecular basis of histone H3K36me3 recognition by the PWWP domain of Brpf1. Nat. Struct. Mol. Biol. **17**: 617–619.

Weiner A., Hsieh T.-H. S., Appleboim A., Chen H. V., Rahat A., Amit I., Rando O. J., Friedman N., 2015 High-resolution chromatin dynamics during a yeast stress response. Molecular Cell **58**: 371–386.

Wu H., Zeng H., Lam R., Tempel W., Amaya M. F., Xu C., Dombrovski L., Qiu W., Wang Y., Min J., 2011 Structural and histone binding ability characterizations of human PWWP domains. PLoS ONE **6**: e18919.

Xue-Franzén Y., Henriksson J., Bürglin T. R., Wright A. P. H., 2013 Distinct roles of the Gcn5 histone acetyltransferase revealed during transient stress-induced reprogramming of the genome. BMC Genomics **14**: 479.

Figure S1

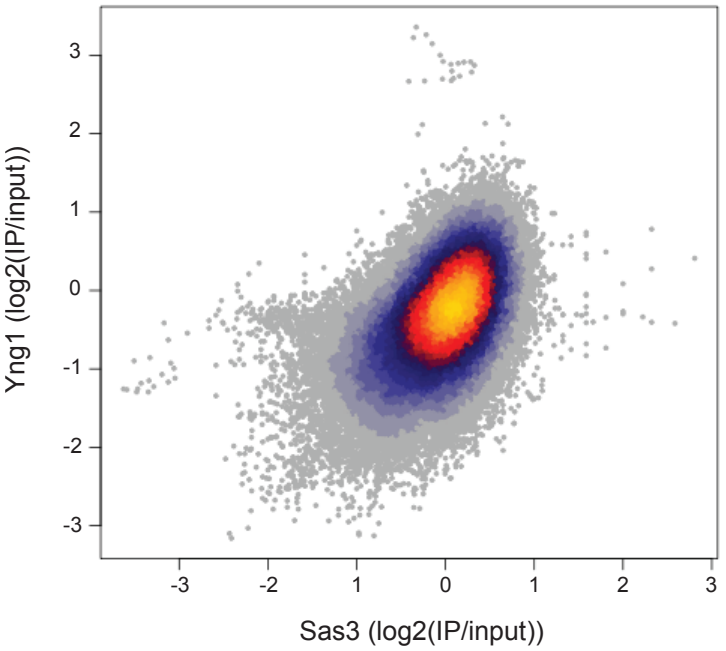

Figure S2

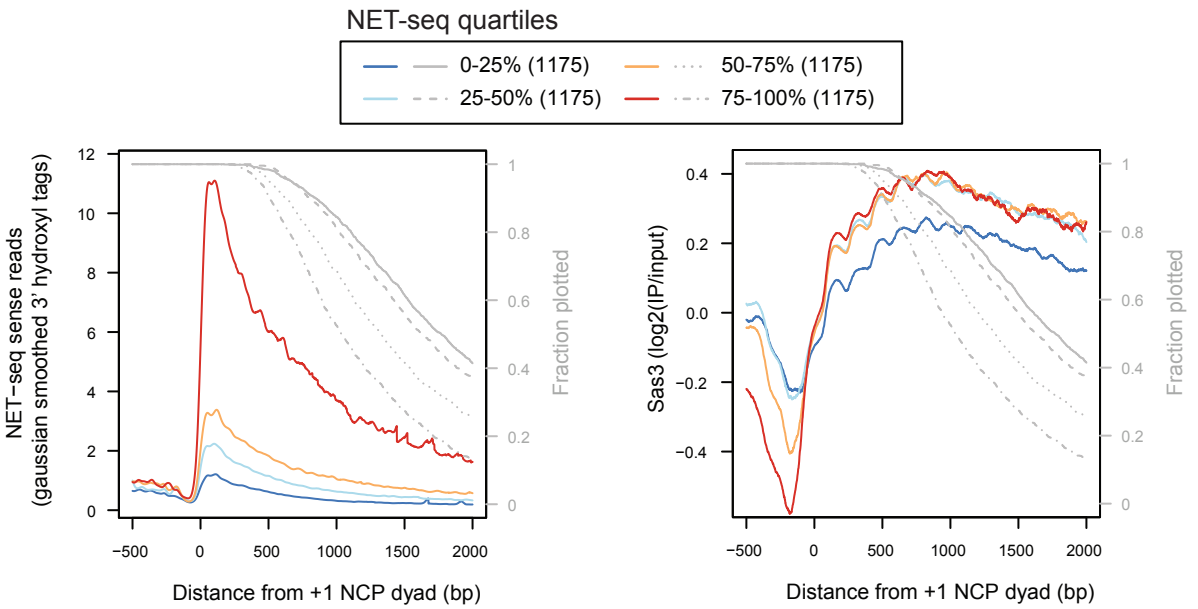
NET-seq quartiles
0-25% (1175)
25-50% (1175)
50-75% (1175)
75-100% (1175)
NET−seq sense reads
(gaussian smoothed 3' hydroxyl tags)
Fraction plotted
Distance from +1 NCP dyad (bp)
Sas3 (log2(IP/input)
Fraction plotted
Distance from +1 NCP dyad (bp)

Figure S3

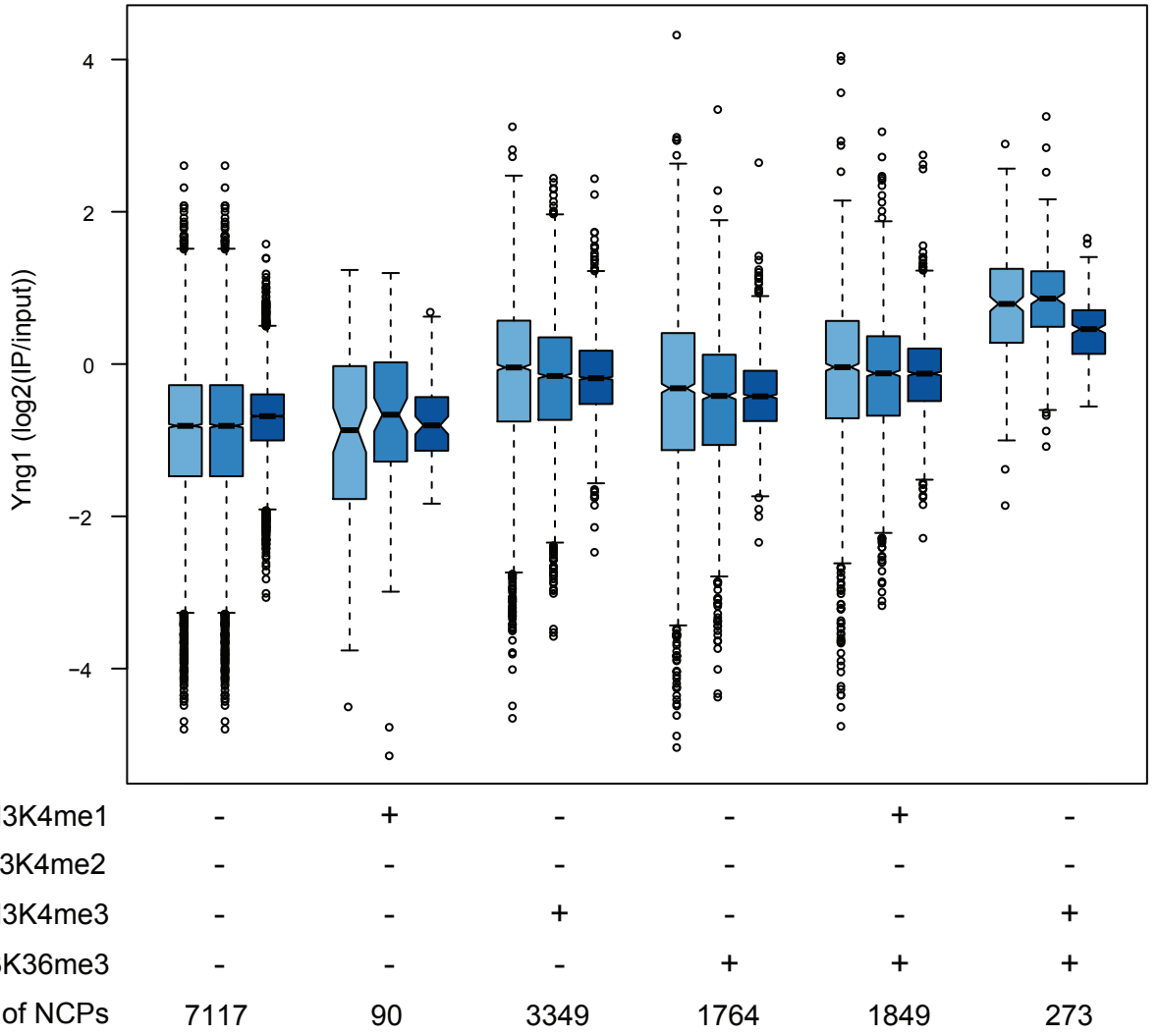
Yng1 (log2(IP/input))
4
2
0
−2
−4
H3K4me1 - + - - + -
H3K4me2 - - - - - -
H3K4me3 - - + - - +
H3K36me3 - - - + + +
# of NCPs 7117 90 3349 1764 1849 273

Figure S4

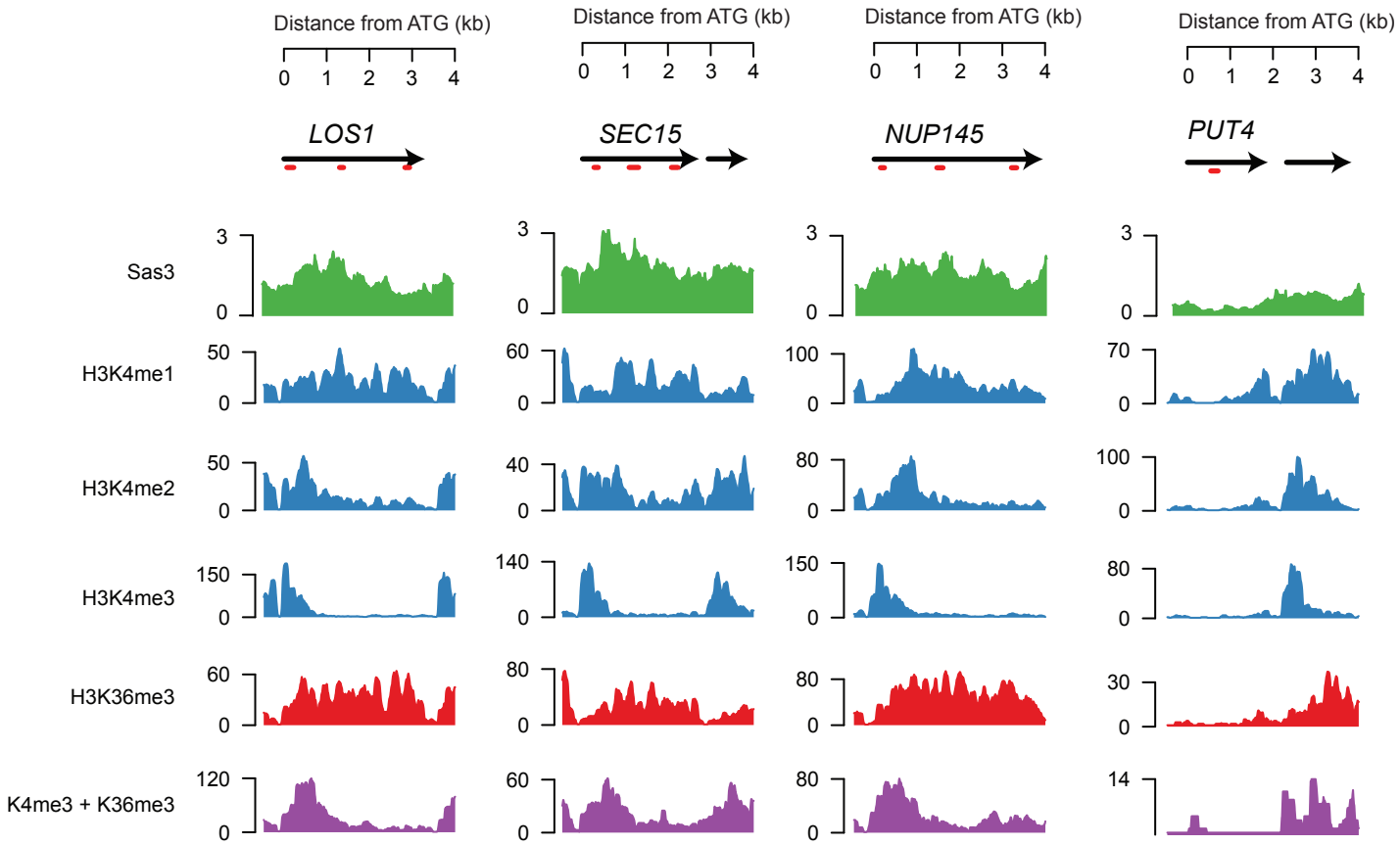
Distance from ATG (kb)
0 1 2 3 4
LOS1
SEC15
NUP145
PUT4
Sas3
H3K4me1
H3K4me2
H3K4me3
H3K36me3
K4me3 + K36me3
3
0
50
60
100
70
40
80
150
140
120
30
14

Figure S5

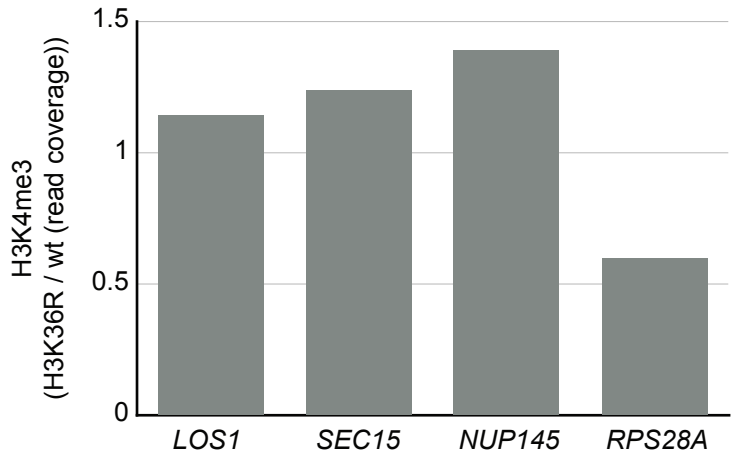
H3K4me3
(H3K36R / wt (read coverage))
1.5
1
0.5
0
LOS1
SEC15
NUP145
RPS28A

Figure S6

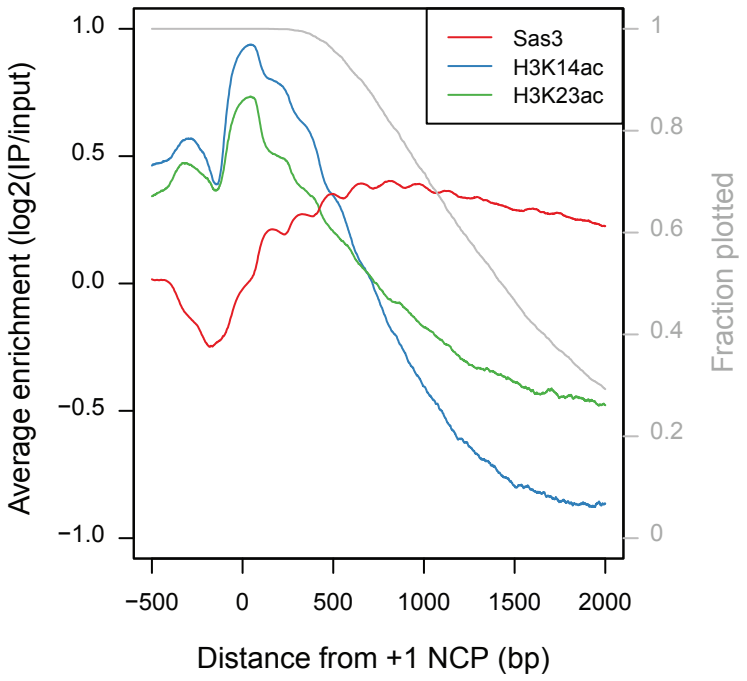
Sas3
H3K14ac
H3K23ac
Average enrichment (log2(IP/input))
Fraction plotted
Distance from +1 NCP (bp)
1.0
0.5
0.0
−0.5
−1.0
1
0.8
0.6
0.4
0.2
0
−500
0
500
1000
1500
2000

Figure S7

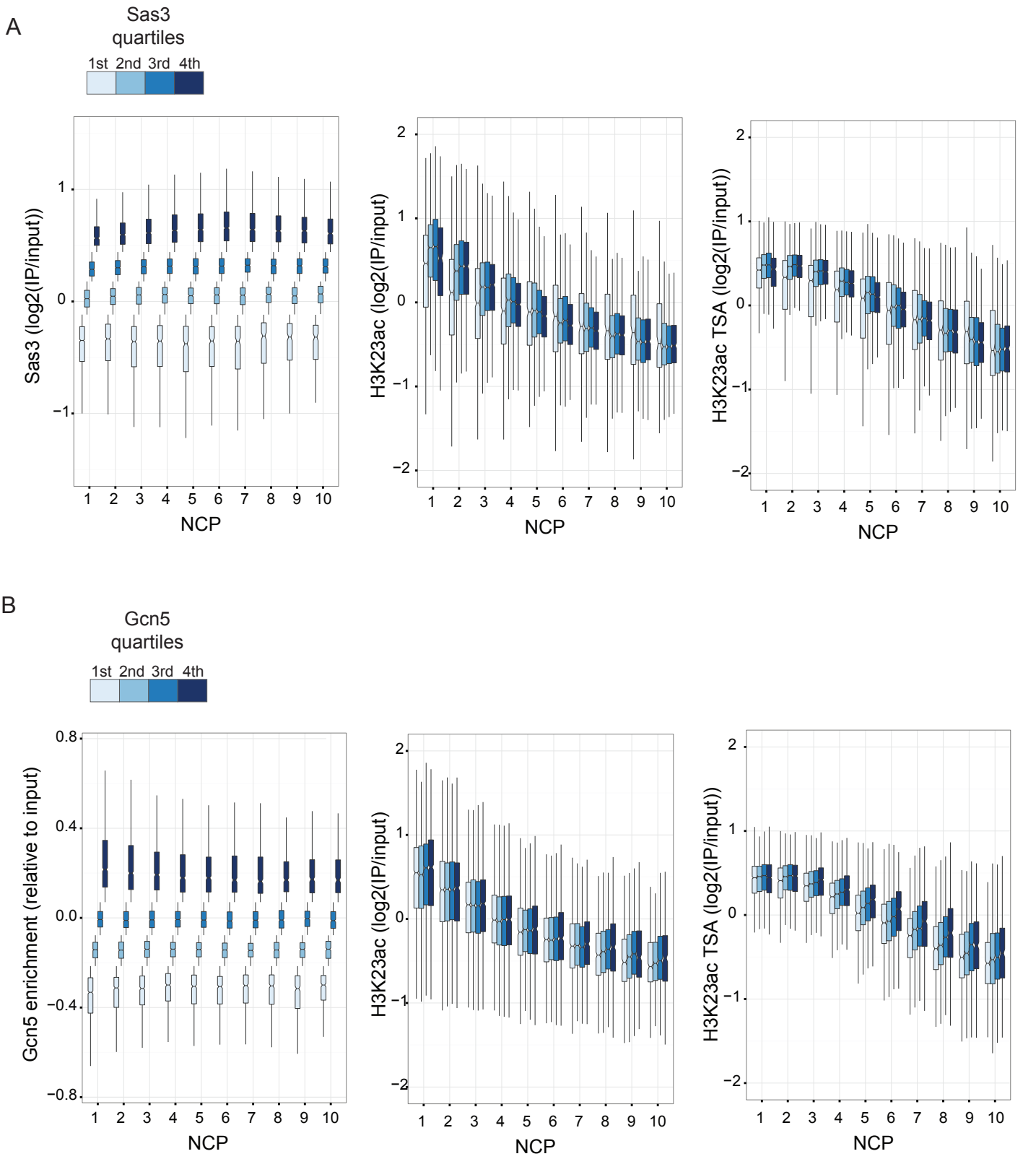
A
Sas3
quartiles
1st 2nd 3rd 4th
Sas3 (log2(IP/input))
H3K23ac (log2(IP/input)
H3K23ac TSA (log2(IP/input))
NCP
B
Gcn5
quartiles
1st 2nd 3rd 4th
Gcn5 enrichment (relative to input)
H3K23ac (log2(IP/input)
H3K23ac TSA (log2(IP/input))
NCP

Figure S8

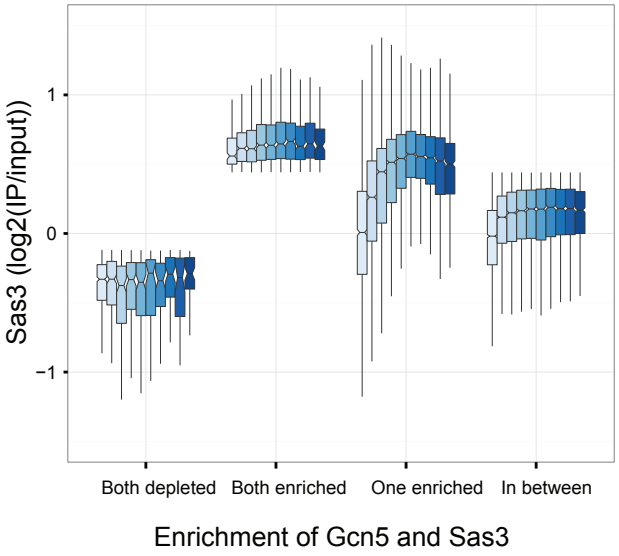
Sas3 (log2(IP/input))
1
0
−1
Both depleted
Both enriched
One enriched
In between
Enrichment of Gcn5 and Sas3

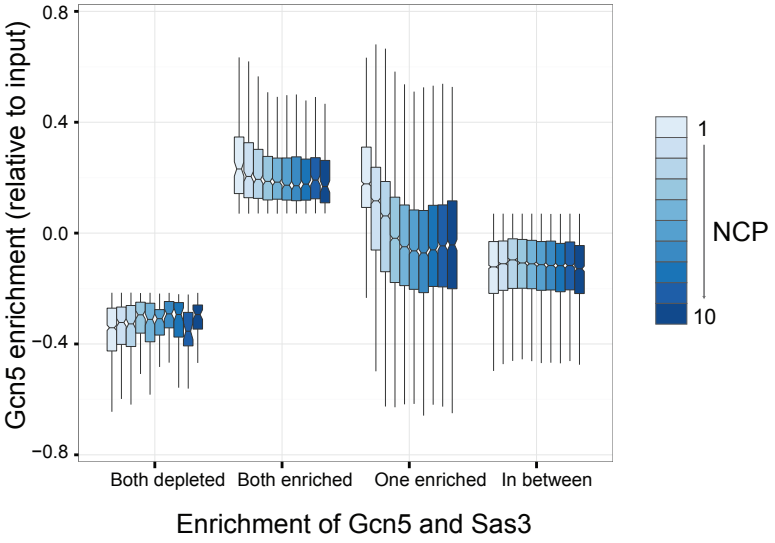
Gcn5 enrichment (relative to input)
0.8
0.4
0.0
−0.4
−0.8
Both depleted
Both enriched
One enriched
In between
Enrichment of Gcn5 and Sas3
1
NCP
10

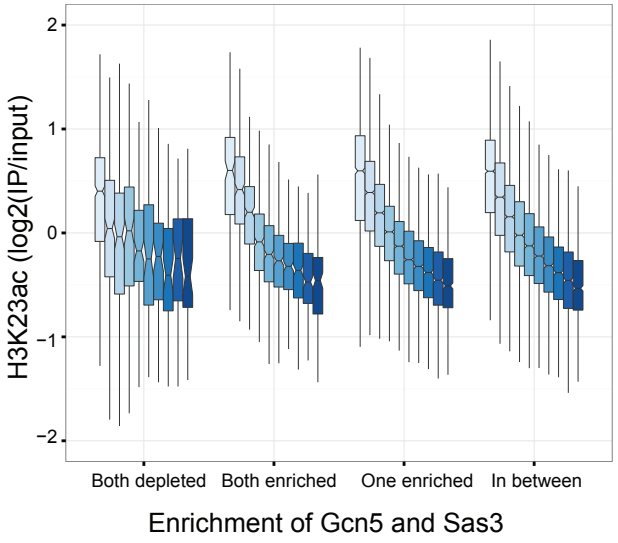
H3K23ac (log2(IP/input))
2
1
0
−1
−2
Both depleted
Both enriched
One enriched
In between
Enrichment of Gcn5 and Sas3

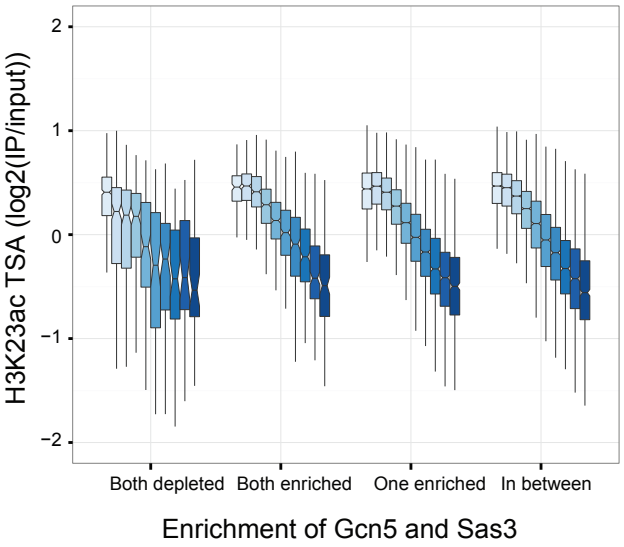
H3K23ac TSA (log2(IP/input))
2
1
0
−1
−2
Both depleted
Both enriched
One enriched
In between
Enrichment of Gcn5 and Sas3